Clays and Clay Minerals, Vol. 34, No. 1, 53–68, 1986.

POLYTYPISM OF MICAS. III. X-RAY DIFFRACTION IDENTIFICATION

Z. WEISS

Coal Research Institute, 716 07 Ostrava-Radvanice
Czechoslovakia

A. WIEWIÓRA

Institute of Geological Sciences, Polish Academy of Sciences
02 089 Warszawa, Poland

Abstract—Classification and identification criteria of maximum-degree-of-order (MDO) polytypes of homo- and meso-octahedral micas based on the distribution of the intensities of 20*l* (13*l*) and 02*l* reflections are proposed. Calculated $|F(20l)|^2$ and $|F(02l)|^2$ values for single crystals of micas with different compositions are given for one-, two-, and three-layer polytypes. Transmission powder diffractometry is proposed as a suitable method for the identification of the different groups of mica polytypes from polycrystalline specimens. Calculated powder patterns and the characteristic properties of the diffraction patterns of random and highly oriented aggregates are employed for identification purposes. The individual MDO polytypes are designated by generalized Ramsdell symbols which also contain information about their position in the classification system.

Key Words—Crystal structure, Mica, Order-disorder, Polytype, Single crystal X-ray diffraction, X-ray powder diffraction.

Resümee—Klassifikations und Identifikationskriterien für alle maximaler Ordnungsgrad (MOG) Polytype von homo- und meso-oktaedrischen Glimmern, die auf den Intensitätenverteilungen von 20*l* (13*l*) und 02*l* Reflexen beruhen, wurden ausgearbeitet. Die berechneten $|F(20l)|^2$ und $|F(02l)|^2$ Werte für Glimmereinkristalle mit variabler Zusammensetzung und für alle Ein-, Zwei-, und Dreischicht-Polytypen sind angeführt. Als geeignete Methode zur Identifikation von verschiedenen Glimmergruppen in ihren polykristallinen Proben ist Transmissions-Diffraktometrie vorgeschlagen. Der Artikel enthält auch berechnete Pulverdiagramme und ihre Identifikations-charakteristische Eigenschaften für sowohl statistisch- als auch hochorientierte Aggregate. Die einzelnen MOG Polytype sind gekennzeichnet durch verallgemeinerte Ramsdellsche Symbole, die auch Information über ihre Stellung in dem Klassifikationssystem enthalten.

INTRODUCTION

In a recent publication (Ďurovič *et al.*, 1984) a classification system for mica polytypes was presented. This system is based on an order-disorder (OD) model of mica structures with ideal ditrigonalization of their tetrahedral sheets—the so-called Radoslovich model (Backhaus and Ďurovič, 1984). It is closely related to characteristic properties of X-ray diffraction patterns of individual mica polytypes because it is based on the following fundamental geometrical characteristics of their structures:

(1) *Superposition structure*—defined according to the OD theory as a hypothetical structure in which all possible positions of all OD layers are realized simultaneously (cf. Backhaus and Ďurovič, 1984). It is by definition three-dimensionally periodic, and, because its basic vector **B** in micas is *b*/3, it corresponds to sharp reflections with k = 3n (orthogonal indexing). All mica polytypes belonging to the same family (i.e., that have the same chemical composition and symmetry of their octahedral sheets) in which all the interlayer cations are octahedrally coordinated, have the same superposition structure and are said to belong to subfamily A. Their fully descriptive polytype symbols (Dornberger-Schiff *et al.*, 1982) contain orientational characters, all of the same parity. The remaining polytypes of the family have all their interlayer cations in a trigonal prismatic coordination and are said to belong to subfamily B. The parity of orientational characters related to individual mica layers in their structures regularly alternates. An analogous parity rule holds also for the characters in the corresponding symbols proposed by Ross *et al.* (1966) in that only even-numbered characters apply to subfamily A and only odd-numbered characters apply to subfamily B. It follows that the X-ray diffraction patterns of all polytypes of the same subfamily have the same characteristic subset of sharp reflections with k = 3n and the same *XZ* projection of their structures.

(2) YZ *projection of the structure.*—All polytypes of the same family which have the same *YZ* projection have also the same set of the 0k*l* reflections in their

X-ray diffraction patterns. These reflections (except k = 3n) are sharp only for periodic polytypes; for non-periodic polytypes they appear as diffuse streaks, or they may be smeared-out completely.

From the geometrical considerations it follows that these two characteristics suffice to characterize unambiguously any polytype. Thus, it is necessary only to inspect reflections with k = 3n to identify the subfamily and then the reflections 0k*l* (k ≠ 3n) to determine the polytype within it. It is the aim of the present paper to describe in detail how this can be done.

Reflections with k = 3n are sharp for all members of a subfamily, regardless of whether they are periodic (ordered) or non-periodic (disordered). Thus, the subfamily can always be determined. On the other hand, any periodic member has its own *YZ* projection and consequently its own characteristic set of 0k*l* (k ≠ 3n) reflections. Of a theoretically infinite number of periodic polytypes from a given subfamily, however, only the polytypes with maximum degree of order (MDO) will be dealt with in this paper. These are the polytypes containing the smallest possible number of kinds of triples, quadruples etc. of OD layers (for their derivation in micas, see Backhaus and Ďurovič, 1984) and, as shown by Ďurovič *et al.* (1984) they are most frequently encountered in natural and synthetic micas.

The three octahedral positions M(1), M(2), and M(3) in the octahedral sheet of a mica polytype can be occupied in different ways. If all positions are occupied by the same cation, one speaks of a homo-octahedral family (commonly containing trioctahedral polytypes), and 6 non-equivalent MDO polytypes exist for it. If two sites are occupied by the same cation and the third by a different cation, a meso-octahedral family results (if the third position is a void, dioctahedral polytypes result), and 14 non-equivalent MDO polytypes exist for it. Finally, if all three sites are occupied by three different cations in an ordered manner, a hetero-octahedral family with 36 non-equivalent MDO polytypes results.

The three octahedral positions can be occupied in the meso-octahedral family in three, and in the hetero-octahedral family, in six different ways. Thus, three meso-octahedral and six hetero-octahedral polytypes can, in general, be assigned to one homo-octahedral polytype. All these polytypes have the same framework of all atoms except those that are octahedrally coordinated, which have similar basic vectors. Their X-ray diffraction patterns are also closer to one another than to those of other polytypes. These relations have been called the *relations of homomorphy.*

All MDO polytypes of a family which have the same *YZ* projection are said to belong to the same MDO group. Five, eleven, and thirty MDO groups exist for homo-, meso-, and hetero-octahedral micas, respectively. Their homomorphic relations are shown in Table 4 of Ďurovič *et al.* (1984) and are useful when identifying polytypes.

GENERALIZED RAMSDELL NOTATION

The relations of homomorphy indicate that the three meso-octahedral and the six hetero-octahedral mica polytypes related to one homo-octahedral family, may have the same number of layers per identity period. They commonly belong to the same crystal system and thus they may have the same Ramsdell symbol. It is, of course, possible to distinguish between them by using their respective fully descriptive polytype symbols. This distinction may not always be practical, and hence it may be advantageous to generalize the popular and widely used Ramsdell symbols, not just by formal subscripts but by identifiers which convey the position of a polytype in the classification system and the relations of homomorphy.

Table 1 is a "cross-reference" classification table for homo- and meso-octahedral mica polytypes. This table differs from Table 4 of Ďurovič *et al.* (1984) not only by its deletion of the hetero-octahedral polytypes but also by its inclusion of the new indicative symbols for the polytypes. As shown in the table, the traditional Ramsdell symbols are combined with the present classification on the basis of the two fundamental structural characteristics mentioned above. The table therefore provides unambiguous polytype designations which are more informative than the traditional symbols alone.

The new notation (valid for all phyllosilicates) consists, as a rule, of three identifiers: The first identifier corresponds essentially to the traditional Ramsdell symbol indicating the number of layers and the crystal class (*A* = triclinic (anorthic),[1] *M* = monoclinic, *O* = orthorhombic, *T* = trigonal, *H* = hexagonal, *R* = rhombohedral). The second is a subscript denoting the subfamily, e.g., $2M_A$, $2M_B$ instead of $2M_1$, $2M_2$ used presently. The third, following the hyphen (-), stands for the appropriate MDO group. One, two, or three numbers may be present, separated by commas (,) for homo-, meso-, and hetero-octahedral families, respectively. The MDO groups in the homo-octahedral family are labelled by roman, and others by arabic numerals; e.g., $1M_A$-I,1 denotes a one-layer monoclinic polytype belonging to the subfamily A and the meso-octahedral MDO group 1 homomorphous to the homo-octahedral group I, that is, the polytype with fully descriptive symbol |3.3|.

The first two identifiers are also meaningful for non-MDO periodic polytypes. Most of these polytypes (Baronnet *et al.*, 1981) belong to subfamily A, and thus the symbols have the form: $3M_A$, $3A_A$, $8M_A$, etc. For highly unprobable polytypes in which both subfamilies intermix, only the first identifiers identical with the traditional Ramsdell symbol can be used. The symbol should also be reduced if diffuse streaks preclude determination of the MDO groups and number of layers by X-ray diffraction methods, but the subfamily can be determined. Such samples should be described merely as a disordered mica polytype of the subfamily A or B. With few exceptions, only these generalized Ramsdell symbols will be used in this paper. The corresponding fully descriptive symbols can be found using Table 1 of the present paper, Table 4 of Ďurovič *et al.* (1984), and Tables 7 and 9 of Backhaus and Ďurovič (1984).

[1] These abbreviations are in keeping with the recent recommendation of the *Ad hoc* Committee on the Nomenclature of Disordered, Modulated and Polytype Structures of the International Union of Crystallography (Guinier *et al.*, 1984).

Table 1. Classification of MDO polytypes of homo-octahedral and meso-octahedral micas.

Homomorph. MDO group	Subfamily A				Subfamily B			
	Homo-octahedral		MDO group	Meso-octahedral	Homo-octahedral		MDO group	Meso-octahedral
I	$1M_A$-I	$(1M)$[1]	1	$1M_A$-I,1	$2O_B$-I	$(2O)$	1	$2O_B$-I,1
			2	$1M_A$-I,2			2	$2O_B$-I,2
			3	$2M_A$-I,3			3	$2O_B$-I,3
II	$2M_A$-II	$(2M_1)$	1	$2M_A$-II,1	—			—
III	—			—	$2M_B$-III	$(2M_2)$	1	$2M_B$-III,1
IV	$3T_A$-IV	$(3T)$	1	$3T_A$-IV,1	—			—
			2	$3T_A$-IV,2				
			3	$3T_A$-IV,3				
V	—			—	$6H_B$-V	$(6H)$	1	$6H_B$-V,1
							2	$6H_B$-V,2
							3	$6H_B$-V,3

[1] Traditional Ramsdell symbols are in parentheses.

PRINCIPLES OF POLYTYPE IDENTIFICATION

The identification of a polytype of a family is influenced not only by the nature of the investigated sample (e.g., disorder), but also by the experimental technique used. Identifications can be made by: (1) refinement of the polytype structure using a complete set of single-crystal data; (2) visual comparison of the observed and calculated distribution of intensities of selected reflections (e.g., $20l$ and $02l$) obtained by single-crystal techniques; and (3) comparison of the observed and calculated X-ray powder diffraction (XRD) patterns of polytypes, possibly using special preparation techniques of polycrystalline samples and special methods of recording the patterns.

The resolution of these methods and also the quality of the results vary considerably. The aim of the present paper is to establish identification criteria for MDO polytypes utilizing their classification elaborated earlier. We shall deal with XRD techniques only, but it is obvious that similar approaches can also be obtained for neutron- and electron-diffraction techniques (see e.g., Zvyagin, 1967; Zvyagin *et al.*, 1979).

The application of approach (1) is obvious and need not be discussed here. It should only be emphasized that this approach is absolutely necessary for the determination of hetero-octahedral polytypes, because the approach requires the refinement of occupancy factors of the three octahedral sites and dimensions of the corresponding coordination octahedra. The following concentrates upon the determination of homo- and meso-octahedral polytypes by means of a comparison of observed XRD data with those calculated for a limited number of model structures—here for MDO polytypes with chemical composition close to that of in-

Table 2. Lattice parameters of the individual MDO polytypes that were used for calculation of their diffraction patterns.[1]

Mica family	Type of lattice	Polytype	a (Å)	b (Å)	c (Å)	α (°)	β (°)	γ (°)	Transformation of indices
Phlogopite	a	$1M_A$-I	5.32	9.21	10.24	90	100	90	$l_6 = 6l + 2h$
	b	$2M_A$-II	5.32	9.21	20.48	90	100	90	$l_6 = 3l + h$
	c	$2M_B$-III	5.32	9.21	21.08	107	90	90	$l_6 = 3l + k$
	d	$3T_A$-IV	5.32	5.32	30.25	90	90	120	$l_6 = 2l$
	e	$2O_B$-I	5.32	9.21	20.17	90	90	90	$l_6 = 3l$
Muscovite	a	$1M_A$-I,1; $1M_A$-I,2	5.19	8.95	10.06	90	100	90	$l_6 = 6l + 2h$
	b	$2M_A$-II,1; $2M_A$-I,3	5.19	8.95	20.12	90	100	90	$l_6 = 3l + h$
	c	$2M_B$-III,1	5.19	8.95	20.69	107	90	90	$l_6 = 3l + k$
	d	$3T_A$-IV,1; $3T_A$-IV,2; $3T_A$-IV,3	5.19	5.19	29.72	90	90	120	$l_6 = 2l$
	e	$2O_B$-I,1; $2O_B$-I,2; $2O_B$-I,3	5.19	8.95	19.81	90	90	90	$l_6 = 3l$
Zinnwaldite	a	$1M_A$-I,1; $1M_A$-I,2	5.30	9.14	10.07	90	100	90	$l_6 = 6l + 2h$
	b	$2M_A$-II,1; $2M_A$-I,3	5.30	9.14	20.14	90	100	90	$l_6 = 3l + h$
	c	$2M_B$-III,1	5.30	9.14	20.75	107	90	90	$l_6 = 3l + k$
	d	$3T_A$-IV,1; $3T_A$-IV,2; $3T_A$-IV,3	5.30	5.30	29.75	90	90	120	$l_6 = 2l$
	e	$2O_B$-I,1; $2O_B$-I,2; $2O_B$-I,3	5.30	9.14	19.83	90	90	90	$l_6 = 3l$

[1] Equations for calculation of l_6 indices (corresponding to the six-layer orthogonal cell) with respect to the different types of lattice geometry are given in last column. The h, k, l indices correspond to the real lattice geometry of the individual MDO polytype.

https://doi.org/10.1346/CCMN.1986.0340107 Published online by Cambridge University Press

Table 3. Calculated $|F|^2$ values for characteristic $20l$ reflections of three different mica families and their classification into A and B subfamilies.[1]

Family	Phlogopite			Zinnwaldite			Muscovite		
Subfamily	A		B	A		B	A		B
$20l$	$+l$	$-l$	$\pm l$	$+l$	$-l$	$\pm l$	$+l$	$-l$	$\pm l$
0			52			3			148
2		478			268			709	
3			593			594			581
4	1041			1428			728		
6			152			317			53
8		24			0			94	
9			351			349			343
10	1197			1589			862		
12			344			565			183
14		54			158			7	
15			115			113			109
16	859			1169			581		
18			414			635			237
20		360			564			201	
21			5			5			5
22	124			247			41		
24			64			157			12
26		183			82			315	
27			868			859			847
28	2677			3113			2198		
30			969			1238			709
32		1015			1282			754	

[1] The indexing and $|F|^2$ values refers to six-layer orthogonal unit cell; $|F|^2$ values are given as $|F|^2/360$. For calculation of indices of A subfamily the equation corresponding to the a-type lattice was used (see Table 2).

Table 4. Calculated $|F|^2$ values for characteristic $02l$ reflections of phlogopite and its classification into MDO groups.[1]

Family	Phlogopite				
MDO group	I	II	III		IV
$02l$	$\pm l$	$\pm l$	$+l$	$-l$	$\pm l$
0	200	50			66
2			32		47
3		63			
4				141	11
6	10	3			3
8			441		54
9		221			
10				163	148
12	711	176			236
14			729		275
15		601			
16				823	243
18	491	122			163
20			66		79
21		103			
22				235	22
24	3	1			1
26			19		2
27		11			
28				7	6
30	12	3			4
32			11		0

[1] The indexing and $|F|^2$ values refers to six-layer orthogonal unit cell; $|F|^2$ values are given as $|F|^2/360$.

Table 5. Calculated $|F|^2$ values for the characteristic $02l$ reflections of zinnwaldite and its classification into MDO groups.[1]

Family	Zinnwaldite							
MDO group	I,1	I,2	I,3	II,1	III,1		IV,1 IV,2	IV,3
$02l$	$\pm l$	$\pm l$	$\pm l$	$\pm l$	$+l$	$-l$	$\pm l$	$\pm l$
0	275	171	166	21			57	91
2					65		59	30
3			5	63				
4						88	8	22
6	32	8	4	1			3	11
8					549		67	36
9			4	222				
10						108	133	184
12	586	778	774	245			258	195
14					605		253	322
15			4	599				
16						962	266	202
18	596	442	438	76			147	198
20					105		91	57
21			4	101				
22						169	17	35
24	0	11	7	9			4	0
26					40		6	0
27			3	11				
28						0	5	13
30	2	22	19	13			7	1
32					27		1	2

[1] The indexing and $|F|^2$ values refers to six-layer orthogonal unit cell; $|F|^2$ values are given as $|F|^2/360$.

https://doi.org/10.1346/CCMN.1986.0340107 Published online by Cambridge University Press

vestigated samples. For this reason a special DIFK (Weiss *et al.*, 1983) program was written to calculate X-ray diffraction patterns of both single crystals and powders. Atomic positions within one OD packet in standard orientation were needed for the input to the program; the other positions were generated automatically using the fully descriptive symbol for the particular polytype. Non-MDO polytypes necessitated a special approach similar to that used for complex polytypes of close-packed structures. This approach will not be dealt with in this paper.

X-RAY DIFFRACTION IDENTIFICATION OF POLYTYPES FROM SINGLE-CRYSTAL DATA

General remarks

As mentioned above, the determination of an MDO polytype requires a determination of its subfamily and its MDO group. Because only two mica subfamilies are possible it sufficed to calculate the distribution of intensities along selected rows of reflections with k = 3n for these two subfamilies only. Experience showed that the 20*l* and 13*l* reflections were best suited for this purpose. Moreover, due to the symmetry of the two superposition structures (subfamily A trigonal, subfamily B hexagonal) and to the validity of Friedel's law, $|F(13l)|^2$ values are related to those of $|F(20l)|^2$. Thus, it was sufficient to calculate the latter values only. For the determination of the MDO group it was necessary to calculate the distribution of intensities along selected rows of reflections 0k*l* (k ≠ 3n) for all MDO groups within the given family. The rows 02*l* and 04*l* are best suited for this purpose, but here again, the symmetry of the corresponding projection may give rise to some simplifications and provide a valuable means for checking the results. Our experience (also with other phyllosilicates) showed that the idealized Pauling model could be used for calculation of identification diagrams which consist of rows of circles whose areas are proportional to the $|F(hkl)|^2$ values of the individual reflections: rows of $|F(20l)|^2$ circles for determination of the subfamily and rows of $|F(02l)|^2$ circles for determination of the MDO group. The sizes of the circles within any such row were normalized to the strongest reflection.

Examples

To demonstrate the identification procedure, three different models of mica families were chosen for the calculation of identification diagrams. Their chemical composition and lattice parameters (Table 2) are artificial, but they approximate typical values in their respective families;

i.e., homo-trioctahedral family (phlogopite)

$$(K_{0.9}Na_{0.1})Mg_{3.0}(Si_{3.0}Al_{1.0})O_{10}(OH)_2,$$

Table 6. Calculated $|F|^2$ values for the characteristic 02*l* reflections of muscovite and its classification into MDO groups.[1]

Family	Muscovite							
MDO group	I,1	I,2	I,3	II,1	III,1		IV,1 IV,2	IV,3
02*l*	±*l*	±*l*	±*l*	±*l*	+*l*	−*l*	±*l*	±*l*
0	442	147	110	0			49	147
2					157		90	7
3			36	62				
4						23	13	52
6	101	35	0	28			12	33
8					754		97	12
9			33	218				
10						36	115	253
12	400	913	882	385			303	133
14					426		224	405
15			21	592				
16						1210	308	142
18	783	385	358	24			128	260
20					189		119	29
21			25	100				
22						87	17	63
24	16	44	20	41			14	5
26					93		17	3
27			22	11				
28						8	8	31
30	3	58	37	48			20	1
32					70		8	11

[1] The indexing and $|F|^2$ values refers to six-layer orthogonal unit cell; $|F|^2$ values are given as $|F|^2/360$.

meso-trioctahedral family (zinnwaldite)

$$(K_{0.9}Na_{0.1})(Al_{1.0}Fe_{1.2}Li_{0.8})(Si_{3.2}Al_{0.8})O_{10}F_2$$

(with the following occupation of octahedral sites: M1 = $Al_{1.0}$ and M1 = M2 = $Fe_{0.6}Li_{0.4}$), and

meso-dioctahedral family (muscovite)

$$(K_{0.9}Na_{0.1})Al_{2.0}(Si_{3.0}Al_{1.0})O_{10}(OH)_2.$$

Table 3 lists the calculated $|F(20l)|^2$ values for the subfamilies A and B. The indexing refers to orthogonal six-layer cell (*a*, *b*, $6c_0$) which is the smallest common supercell for all MDO polytypes. The transformation of indices for the actual lattice geometries is given in Table 2. It can be seen that both subfamilies are readily distinguishable. The calculated $|F(02l)|^2$ values for the identification of MDO groups (except for the MDO group V containing six-layer polytypes which have not yet been observed) are listed in Tables 4–6. The calculations revealed that the complete XRD patterns of the meso-octahedral MDO polytypes $3T_A$-IV,1 and $3T_A$-IV,2 are so similar that it is impossible to distinguish between them visually; the determination of the remaining meso-octahedral MDO groups is less problematic and is easier if the occupancies of two octahedral sites are close to one another and if they differ considerably from the remaining one.

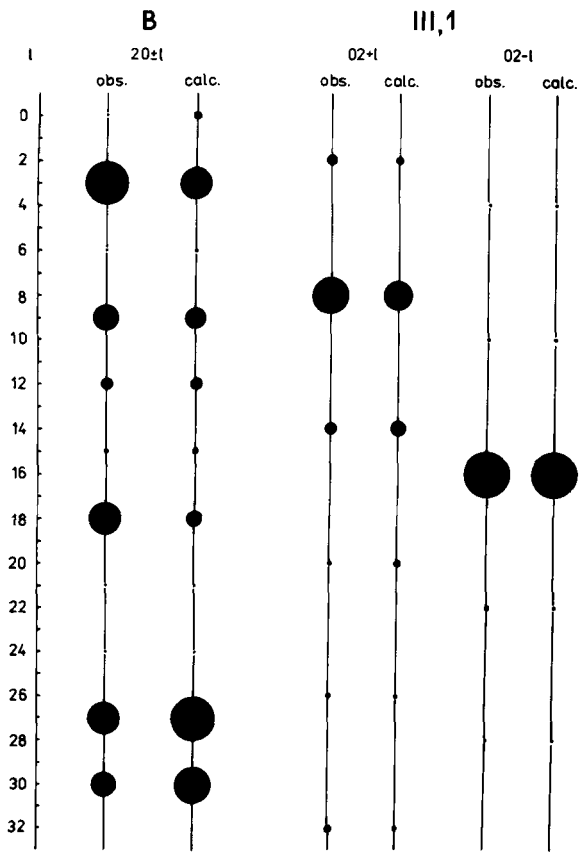

Three mica polytypes with reliably determined and refined structures were chosen to show how the visual-comparison technique works: (1) *Meso-dioctahedral Al-mica* $2M_B$*-III,1* ($2M_2$). The crystal structure of this mica was determined by Zhoukhlistov *et al.* (1973). The characteristic $|F|^2$ values calculated from their data and the theoretical values calculated for the model polytype $2M_B$-III,1 are shown in Figure 1. The determination of the polytype is straightforward. (2) *Hetero-dioctahedral muscovite* $3T_A$*-IV,1,1.* Visual comparison of the characteristic $|F|^2$ values calculated from the data published by Güven and Burnham (1967) with the theoretical values for meso-octahedral muscovites (Figure 2) indicates the MDO polytype $3T_A$-IV,1 or $3T_A$-IV,2. This polytype was to be expected because the structure refinement, suggests that the structure is almost meso-octahedral. The M(1) position is vacant, and the M(2) and M(3) positions contain 11.5 and 12.5 electrons, respectively. (3) *Hetero-trioctahedral zinn-waldite* $1M_A$*-I,2,1.* The crystal structure of this mica was determined by Guggenheim and Bailey (1977).

←

Figure 1. Comparison of the characteristic $|F(20l)|^2$ and $|F(02l)|^2$ values calculated from the structure data published by Zhoukhlistov *et al.* (1973) (obs.) and theoretical values calculated for MDO polytype $2M_B$-III,1 of muscovite (calc.). Indexing refers to the orthogonal six-layer unit cell. $|F|^2$ values are normalized to the strongest diffraction intensity.

Table 7. Calculated absolute powder intensities[1] of selected reflections which are decisive for the identification of subfamilies A and B of the MDO polytypes of phlogopite.[2]

		$1M_A$-I		$2M_A$-II		$3T_A$-IV				$2O_B$-I		$2M_B$-III	
d (Å)	ν_{hkl}	hkl	I_{abs}[1]	hkl	I_{abs}	hkl	I_{abs}	d (Å)	ν_{hkl}	hkl	I_{abs}	hkl	I_{abs}
2.65	85.0	$\bar{2}01$	82	$\bar{2}02$	82	111	246	2.66	90.0	200	10	200	10
		130	164	130	164					130	20	$1\bar{3}2$	20
2.62	80.0	200	173	200	173	$\bar{1}22$	517	2.64	82.5	201	200	201	200
		$\bar{1}31$	344	$\bar{1}32$	344					131	400	$1\bar{3}3$	200
2.51	70.6	$\bar{2}02$	5	$\bar{2}04$	5	114	11		97.5			$1\bar{3}1$	200
		131	6	132	6			2.57	75.2	202	48	202	48
2.44	66.3	201	169	202	169	$\bar{1}25$	506			132	96	130	48
		$\bar{1}32$	337	$\bar{1}34$	337							$1\bar{3}4$	48
2.27	58.4	$\bar{2}03$	6	$\bar{2}06$	6	117	19	2.47	68.4	203	104	203	104
		132	13	134	13					133	208	131	104
2.18	54.9	202	94	204	94	$\bar{1}28$	281					$1\bar{3}5$	104
		$\bar{1}33$	187	$\bar{1}36$	187			2.35	62.2	204	90	204	90
2.00	48.7	$\bar{2}04$	32	$\bar{2}08$	32	11,10	96			134	180	132	90
		133	64	136	64							$1\bar{3}6$	90
1.91	46.0	203	10	206	10	$\bar{1}2,11$	30	2.22	56.6	205	27	205	27
		$\bar{1}34$	20	$\bar{1}38$	20					135	54	133	27
												$1\bar{3}7$	27
								2.09	51.6	206	82	206	82
										136	164	134	82
												$1\bar{3}8$	82

[1] In electron units multiplied by 100, without correction for absorption.

[2] Indexing refers to the actual unit cells of the polytypes (see Table 2). For calculations the idealized symmetry and chemical compositions were used.

https://doi.org/10.1346/CCMN.1986.0340107 Published online by Cambridge University Press

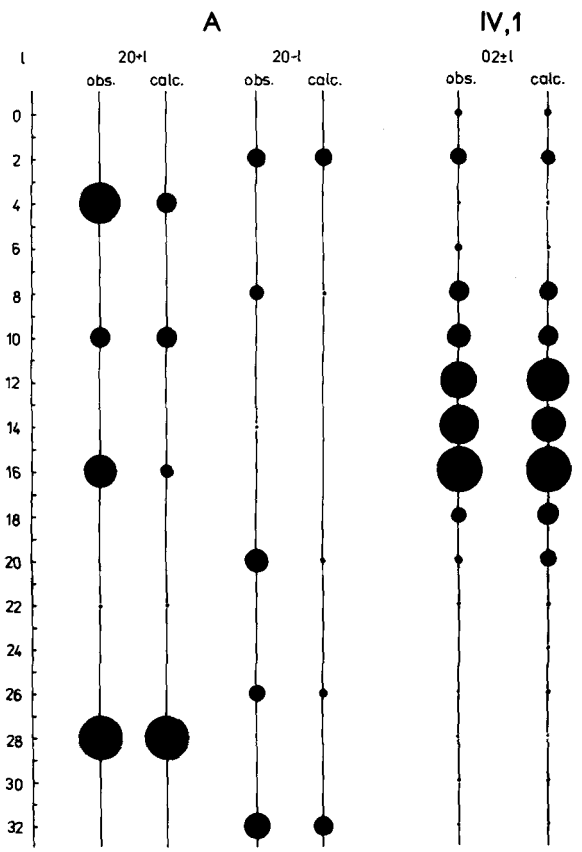

Figure 2. Comparison of the characteristic $|F(20l)|^2$ and $|F(02l)|^2$ values calculated from the structure data published by Güven and Burnham (1967) (obs.) and theoretical values calculated for MDO polytype $3T_A$-IV,1 of muscovite (calc.). Indexing refers to the orthogonal six-layer unit cell. $|F|^2$ values are normalized to the strongest diffraction intensity.

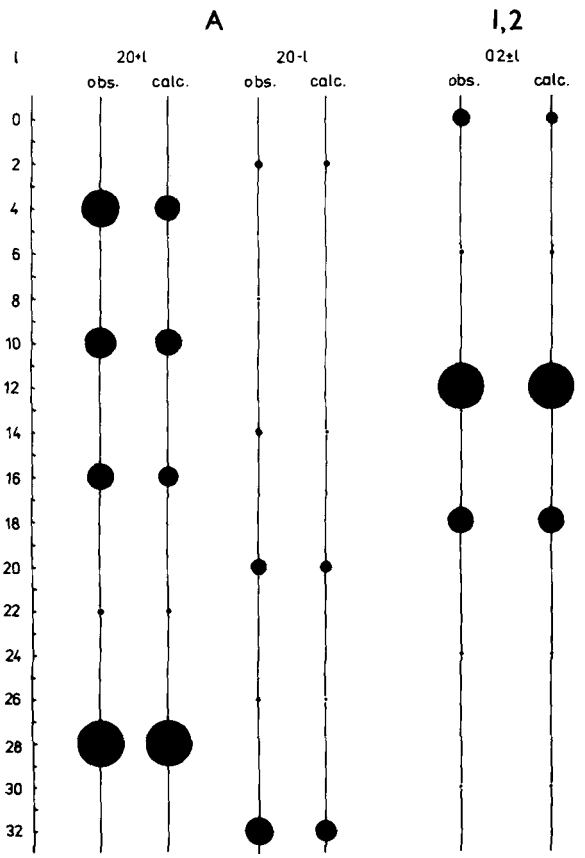

Figure 3. Comparison of the characteristic $|F(20l)|^2$ and $|F(02l)|^2$ values calculated from the structure data published by Guggenheim and Bailey (1977) (obs.) and theoretical values calculated for MDO polytype $1M_A$-I,2 of zinnwaldite (calc.). Indexing refers to the orthogonal six-layer cell. $|F|^2$ values are normalized to the strongest diffraction intensity.

Visual comparison of the characteristic $|F|^2$ values calculated from the published data with theoretical values for model meso-trioctahedral zinnwaldite (Figure 3) indicates the polytype $1M_A$-I,2.

It is interesting to note that even relatively rough structural models (i.e., idealized symmetry, artificial meso-octahedral occupation schemes with M1 = $Al_{1.0}$ and M2 = M3 = $Fe_{0.6}Li_{0.4}$) led to the polytype with non-centrosymmetric mica layers and not to one with centrosymmetric layers $1M_A$-I,1. The symbol of the actual polytype is $1M_A$-I,2,1, and the three octahedral positions are occupied by 15.0, 11.5 and 13.5 electrons, respectively.

From these examples it can be concluded that the visual-comparison technique can be used for the determination of the subfamily as well as for the MDO group of homo- and meso-octahedral mica polytypes, provided that the identification diagrams are calculated for a chemical composition which is similar to that of the investigated samples. From these comparisons it is also apparent that the desymmetrization of the structure causes minor changes in the distribution of the $|F(02l)|^2$ values, but more significant changes in the distribution of the $|F(20l)|^2$ values. These changes were found to be more pronounced in muscovites (e.g., tetrahedral-rotation angles $\alpha = 11.2°$ and $11.8°$ in real structures—examples 1 and 2), than in zinnwaldite with $\alpha = 5.8°$. In these structures relatively good fits between observed intensities and identification diagrams were achieved because the theoretical and real compositions were similar.

IDENTIFICATION OF POLYTYPES FROM X-RAY POWDER DIFFRACTION DATA

General remarks

Identification of mica polytypes using XRD data is more complicated and less effective in comparison with single-crystal methods because: (1) XRD patterns contain, in addition to the 20*l*, 02*l*, and 04*l* reflections, strong 13*l*, 11*l*, 00*l*, and other reflections. The latter

https://doi.org/10.1346/CCMN.1986.0340107 Published online by Cambridge University Press

Table 8. Calculated absolute powder intensities[1] of selected reflections which are decisive for the identification of MDO groups[2] together with overlapping reflections of the MDO polytypes of phlogopite.[3]

d (Å)	ν_{hkl}	$1M_A$-I		$2O_B$-I		$2M_A$-II		$2M_B$-III		$3T_A$-IV	
		hkl	I_{abs}[1]	hkl	I_{abs}	hkl	I_{abs}	hkl	I_{abs}	hkl	I_{abs}
4.61	90.0	020	112	020	112	020	28			$\bar{1}10$	56
				110	55					100	56
4.59	85.6					$\bar{1}11$	148	$1\bar{1}1$	148		
4.55	81.3	110	151			110	38	110	38	101	75
								$0\bar{2}2$	75	$\bar{1}11$	75
4.49	77.1			111	130	021	67				
4.41	73.1	$\bar{1}11$	31			$\bar{1}12$	8	$1\bar{1}2$	8	102	16
								020	16	$\bar{1}12$	16
4.31	69.1					111	2				
4.19	65.5	021	9	022	9	022	2			$\bar{1}13$	5
				112	4					103	5
4.07	61.9					$\bar{1}13$	40	$1\bar{1}3$	40		
3.94	58.7	111	129			112	32	112	32	104	66
								$0\bar{2}4$	66	$\bar{1}14$	66
3.80	55.6			113	326	023	166				
3.67	52.7	$\bar{1}12$	305			$\bar{1}14$	76	$1\bar{1}4$	76	105	153
								022	153	$\bar{1}15$	153
3.53	50.1					113	280	113	280		
3.40	47.6	022	420	024	420	024	104			$\bar{1}16$	210
				114	208					106	210
3.27	45.3					$\bar{1}15$	321	$1\bar{1}5$	321		
3.15	43.2	$1\bar{1}2$	409			114	103	114	103	107	204
								$0\bar{2}6$	204	$\bar{1}17$	204
3.04	41.2			115	550	025	278				
2.92	39.4	$\bar{1}13$	307			$\bar{1}16$	77	$1\bar{1}6$	77	108	153
								024	153	$\bar{1}18$	153
2.82	37.7					115	180	115	180		
2.72	36.1	023	177	026	177	026	44			$\bar{1}19$	89
				116	88					109	89
2.62	34.7					$\bar{1}17$	89	$1\bar{1}7$	89		

[1] In electron units multiplied by 100, without correction for absorption.
[2] Their indices are underlined.
[3] Indexing refers to the actual unit cells of the polytypes (see Table 2). For calculations the idealized symmetry and chemical composition were used.

commonly overlap the former. In addition, the resolution of reflections is poor due also to the special lattice geometry of mica polytypes which can be described in terms of a common six-fold hexagonal cell. (2) The distribution of intensities can be strongly influenced by the texture of the sample, which is commonplace when the classical (reflection arrangement) diffractometer technique is used. This technique enhances the 00*l* reflections that are useless for polytype identification and suppresses reflections that are necessary.

At present, four basic variants of XRD methods are available that yield qualitatively different results concerning identification of polytypes;

(1) A transmission method that uses samples with highly oriented crystallites and axial texture as described by Plançon *et al.* (1982). In this method it is possible to scan along the generating rods of selected (hk) cylinders in reciprocal space. Thus, a scan along the (20,13) and (11,02) rods provides data for the determination of the subfamily and the MDO group, respectively. Although the preparation of a textured sample is relatively simple, this method necessitates a diffractometer without a θ-2θ coupling. Samples are examined by a step-scan technique where the settings for the sample and the counter must be calculated in advance.

(2) A transmission method that uses samples with random orientation of crystallites. This method can be realized by using either diffractometer or film techniques, such as Guinier method, classical Debye-

Table 9. Calculated absolute powder intensities[1] of selected reflections which are decisive for the identification of subfamilies A and B of the MDO polytypes of muscovite.[2]

d (Å)	ν_{hkl}	$1M_A$-I,1 $1M_A$-I,2 hkl	I_{abs}[1]	$2M_A$-I,3 $2M_A$-II,1 hkl	I_{abs}	$3T_A$-IV,1 $3T_A$-IV,3 hkl	I_{abs}	d (Å)	ν_{hkl}	$2O_B$-I,1 $2O_B$-I,2 $2O_B$-I,3 hkl	I_{abs}	$2M_B$-III,1 hkl	I_{abs}
2.58	85.0	$\bar{2}01$	132	$\bar{2}02$	132	111	395	2.59	90.0	200	28	200	28
		130	263	130	263					130	56	$1\bar{3}2$	56
2.55	80.1	200	132	200	132	$\bar{1}22$	392	2.57	82.5	201	105	201	105
		$\bar{1}31$	260	$\bar{1}32$	260					131	210	$1\bar{3}3$	105
2.45	70.8	$\bar{2}02$	15	$\bar{2}04$	15	114	45		97.5			$1\bar{3}1$	105
		131	30	132	30			2.50	75.3	202	9	202	9
2.37	66.4	201	133	202	133	$\bar{1}25$	396			132	18	130	9
		$\bar{1}32$	263	$\bar{1}34$	263							$1\bar{3}4$	9
2.21	58.6	$\bar{2}03$	1	$\bar{2}06$	1	117	3	2.40	68.6	203	54	203	54
		132	2	134	2					133	108	131	54
2.13	55.1	202	69	204	69	$\bar{1}28$	206					$1\bar{3}5$	54
		$\bar{1}33$	137	$\bar{1}36$	137			2.29	62.4	204	26	204	26
1.95	48.9	$\bar{2}04$	20	$\bar{2}08$	20	11,10	59			134	52	132	26
		133	39	136	39							$1\bar{3}6$	26
1.87	46.2	203	4	206	4	$\bar{1}2,11$	11	2.16	56.8	205	14	205	14
		$\bar{1}34$	7	$\bar{1}38$	7					135	28	133	14
												$1\bar{3}7$	14
								2.03	51.8	206	26	206	26
										136	52	134	26
												$1\bar{3}8$	26

[1] In electron units multiplied by 100, without correction for absorption.
[2] Indexing refers to the actual unit cells of the polytypes (see Table 2). For calculations the idealized symmetry and chemical composition were used.

Scherrer method, etc. The preparation of samples is more difficult than in (1), but the method yields a diffraction pattern with all reflections, commonly overlapping, but with correct relative intensities.

(3) A transmission method that uses samples with highly oriented crystallites and axial texture as described by Krinari (1975). This method makes it possible to obtain a diffraction pattern with enhanced intensities of reflections belonging to certain cones (see below). An enhancement of the superposition-structure and MDO group reflections is possible. The most important advantage of this method is the possibility of using a conventional diffractometer with a θ-2θ coupling.

(4) The classical "reflection" diffractometric method that uses textured sample is useless, as mentioned above. It can be improved by using a sample with random orientations of crystallites. The preparation of such a sample, however, is more difficult than the preparation of transparent samples as in (2).

The identification proper can then be made by a comparison of experimental patterns with those calculated for the appropriate technique and chemical composition.

Only the identification of mica polytypes using variants (2) and (3) are discussed below. They employ experimental conditions that are commonplace in most laboratories and that yield satisfactory results.

Calculation of XRD patterns

The XRD intensity can be expressed by the following formula

$$I(hkl) = K \cdot V^{-2} \cdot Lp \cdot m \cdot |F|^2 \cdot A \cdot E, \qquad (1)$$

where K is a constant that includes only physical and instrumental constants, V is the volume of unit cell, Lp, m, and $F(hkl)$ are the Lorentz-polarization factor, multiplicity factor, and structure factor, respectively, A is an absorption factor, and E is an enhancement factor. The last two factors are of special importance.

Absorption factor. The absorption correction in the transmission method is given by the general formula from Crohe (1976):

$$A = \frac{1}{\mu}\left[\frac{\sin\psi}{\sin\phi - \sin\psi}\right] \cdot \left[\exp\left(-\frac{\mu t}{\sin\phi}\right) - \exp\left(-\frac{\mu t}{\sin\psi}\right)\right], \qquad (2)$$

where $\phi = \nu_0 + \theta$ is the angle between the incident beam and the sample plane, ν_0 is the initial position angle of the sample, adjusted when the detector counter stays at $2\theta = 0°$, $\psi = \phi - 2\theta$, t is the thickness of the sample, and μ is the linear-attenuation coefficient.

https://doi.org/10.1346/CCMN.1986.0340107 Published online by Cambridge University Press

Table 10. Calculated absolute powder intensities[1] of selected reflections which are decisive for the identification of MDO groups[2] together with overlapping reflections of the MDO polytypes of muscovite.[3]

d (Å)	ν_{hkl}	hkl	$1M_A$-I,1 I_{abs}[1]	$1M_A$-I,2 I_{abs}	hkl	$2O_B$-I,1 I_{abs}	$2O_B$-I,2 I_{abs}	$2O_B$-I,3 I_{abs}	hkl	$2M_A$-I,3 I_{abs}	$2M_A$-II,1 I_{abs}	hkl	$2M_B$-III,1 I_{abs}	hkl	$3T_A$-IV,1 I_{abs}	$3T_A$-IV,3 I_{abs}
4.48	90.0	020	268	90	020	268	90	67	020	67				$\bar{1}10$	45	134
					110		181	135						100	45	134
	85.7								$\bar{1}11$	45	160	$1\bar{1}1$	160			
4.43	81.4	110	26	318					110	274	196	110	196	101	159	13
												$0\bar{2}2$	13	$\bar{1}11$	159	13
4.37	77.4				111	144	144	229								
					021			42	021	42	72					
4.30	73.2	$\bar{1}11$	172	46					$\bar{1}12$	5	20	$1\bar{1}2$	20	102	23	86
												020	86	$\bar{1}12$	23	86
4.20	69.3								111	38	2					
4.08	65.7	021	100	36	022	100	36		022		28			$\bar{1}13$	18	50
					112	56	124	52						103	18	50
3.97	62.1								$\bar{1}13$	33	44	$1\bar{1}3$	44			
3.84	58.9	111	30	254					112	224	150	112	150	104	127	15
												$0\bar{2}4$	15	$\bar{1}14$	127	15
3.71	55.9				113	360	360	410								
					023			27	023	27	179					
3.58	52.9	$\bar{1}12$	574	260					$\bar{1}14$	234	12	$1\bar{1}4$	12	105	130	287
												022	287	$\bar{1}15$	130	287
3.45	50.3								113	23	303	113	303			
3.32	47.9	022	260	590	024	260	590	574	024	574	249			$\bar{1}16$	295	130
					114	510	174	132						106	295	130
3.20	45.5								$\bar{1}15$	18	348	$1\bar{1}5$	348			
3.09	43.4	112	660	366					114	350	34	114	34	107	183	330
												$0\bar{2}6$	330	$\bar{1}17$	183	330
2.97	41.5				115	606	606	636								
					025			15	025	15	300					
2.86	39.6	$\bar{1}13$	196	428					$\bar{1}16$	414	180	$1\bar{1}6$	180	108	214	98
												024	99	$\bar{1}18$	214	98

[1] In electron units multiplied by 100, without correction for absorption.
[2] Their indices are underlined.
[3] Indexing refers to the actual unit cells of the polytypes (see Table 2). For calculations the idealized symmetry and chemical composition were used.

Enhancement factor. It is well known that the diffraction condition for a set of hk*l* planes of a crystal is fulfilled if their common normal bisects the angle $180° - 2\theta°$ formed by the incident and the diffracted beam; hence, the θ-2θ geometry used in current commercial diffractometers. Deviations from this geometry influence the intensity of the diffracted beam which decreases with increasing angle between the normal to hk*l* planes and the bisectrice.

In a highly oriented sample that has Z^* as a texture axis, the hk*l* normals of individual crystallites with random azimuthal orientation form a conus co-axial with Z^*. The hk0 normals lie in a plane which can be considered as a special case of the above conuses. Here, the corresponding hk0 planes evidently form a *zone*. It follows that the diffraction condition is most favorable for these zonal reflections if $\nu_0 = 90°$. The intensities of all other reflections during the following θ-2θ scan were reduced by the factor E whose general form, determined empirically by the present authors, reads:

$$E = \exp[-g \cdot \sin^2(\nu_0 - \nu_{hkl})], \quad (3)$$

where g is a coefficient characterizing the degree of orientation of the aggregate and ν_{hkl} is the angle between Z^* and the surface line of the conus formed by all hk*l* normals. For randomly oriented crystallites, g = 0; hence E = 1.

If $\nu_0 \neq 90°$ (oblique-texture geometry), another conus of hk*l* planes is in the most favorable diffraction position (E = 1). The corresponding hk*l* planes can be

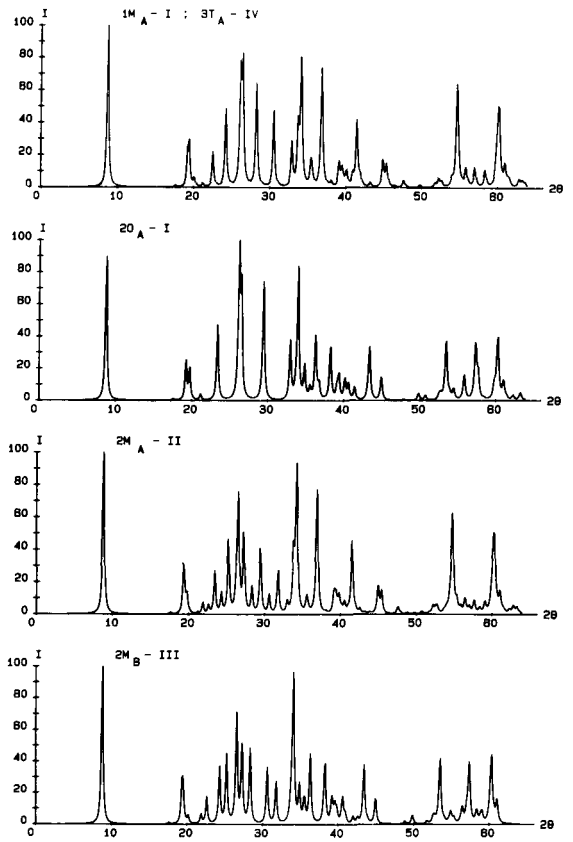

Figure 4. Calculated powder diffraction patterns of MDO polytypes of phlogopite (conditions: diffractometer, transmission, Cu-radiation, random-orientation geometry). Idealized symmetry and chemical composition were used for the calculation.

determined by using the lattice geometry of the investigated substance. The reduction of intensities ($E < 1$) of the remaining reflections depends again on the difference, $\nu_0 - \nu_{hkl}$.

From the above considerations, the DIFK computer program (Weiss *et al.,* 1983) was modified, and the diffraction profile was approximated by the following Lorentz function:

$$J(\theta) = \sum \frac{a_1 I(hkl)}{\pi H_i(\theta)} \left[1 + a_2 \left(\frac{\theta - \theta_i}{H_i(\theta)} \right)^2 \right]^{-a_3}, \qquad (4)$$

where $I(hkl)$ is the intensity of the reflection at the position θ_i, $H_i(\theta)$ is the half-width, a_1, a_2, a_3 are optional coefficients, and Σ is the sum over all contributing reflections (Weiss *et al.,* 1983).

Identification powder patterns

Random-orientation geometry. To obtain a general survey of identification powder patterns, XRD patterns for all homo- and meso-octahedral MDO mica polytypes (except for six-layer polytypes), using idealized Pauling models of their structures, were calculated. Representative phlogopites (homo-octahedral) and muscovites (meso-octahedral) whose chemical compositions and lattice parameters were given above, were selected for study. Calculated absolute intensities (in electron units, without correction for absorption) of selected reflections which are decisive for the identification of subfamilies and MDO groups together with reflections that commonly overlap the former are given

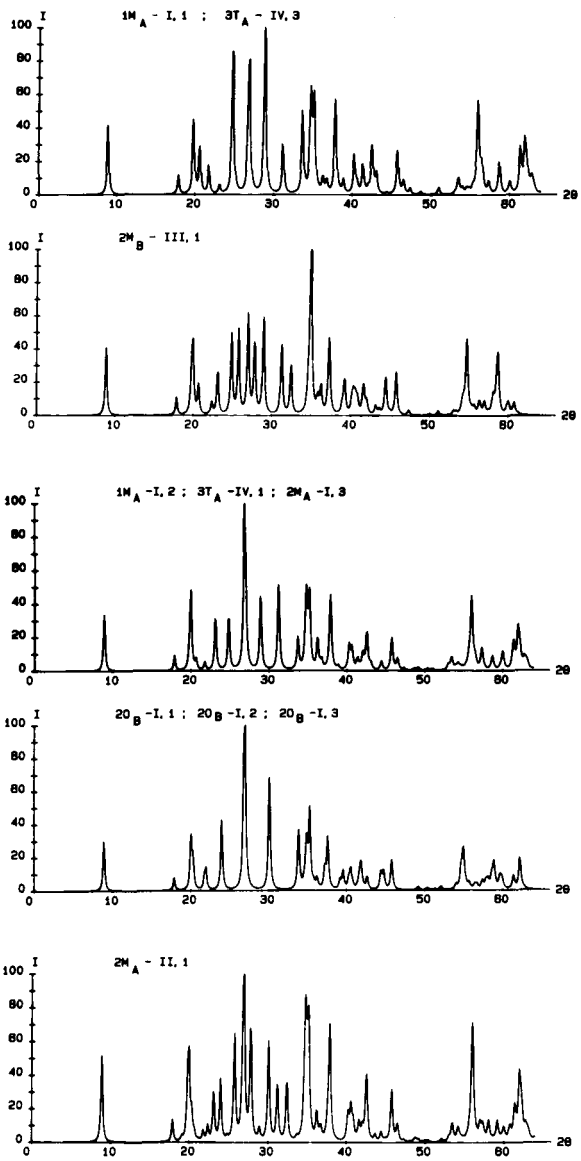

Figure 5. Calculated powder diffraction patterns of MDO polytypes of muscovite (conditions: diffractometer, transmission, Cu-radiation, random-orientation geometry). Idealized symmetry and chemical composition were used for the calculation.

https://doi.org/10.1346/CCMN.1986.0340107 Published online by Cambridge University Press

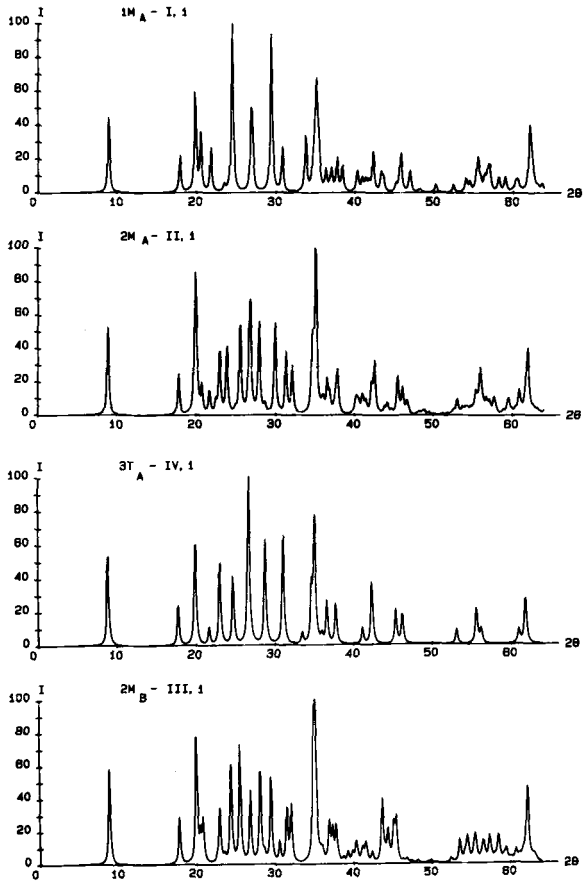

Figure 6. Calculated powder diffraction patterns of selected MDO polytypes of muscovite (conditions: diffractometer, transmission, Cu-radiation, random-orientation geometry). The real geometry of crystal structures given by Sidorenko *et al.* (1975), Güven (1971), Zhoukhlistov *et al.* (1973) and Güven and Burnham (1967) for $1M_A$-I,1, $2M_A$-II,1, $2M_B$-III,1, $3T_A$-IV,1, respectively and idealized chemical composition were used for the calculation.

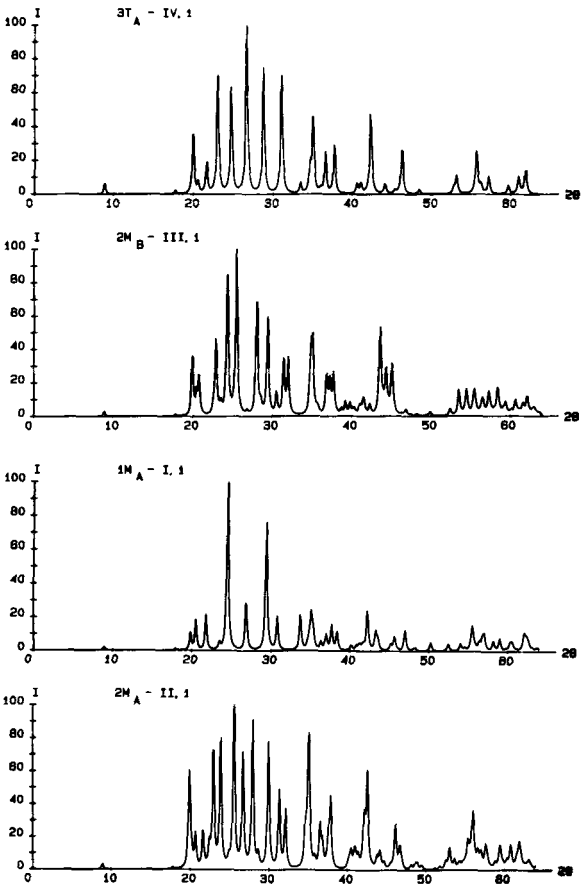

Figure 7. Calculated powder oblique texture diffraction patterns for $\nu_0 = 55°$ (conditions: diffractometer, transmission, Cu-radiation, oblique-texture geometry) of selected MDO polytypes of muscovite. The real geometry of crystal structures (as well as in Figure 6) and idealized chemical composition were used for the calculation.

in Tables 7–10. Calculated identification powder patterns (including all possible reflections) of phlogopite and muscovite polytypes are given in Figures 4 and 5. Some MDO polytypes have *practically indistinguishable* XRD powder patterns, including:

(1) homo-octahedral MDO polytypes (phlogopite) $1M_A$-I and $3T_A$-IV, and

(2) meso-octahedral MDO polytypes (muscovite) $1M_A$-I,1 and $3T_A$-IV,3; $1M_A$,-I,2, $3T_A$-IV,1, and $2M_A$-I,3; $2O_B$-I,1, $2O_B$-I,2, and $2O_B$-I,3. (XRD pattern for the polytype $3T_A$-I,2 was not calculated because, as mentioned above, even its single-crystal pattern was indistinguishable from that of $3T_A$-I,1. Thus, there was no possibility of distinguishing these two polytypes by their XRD powder patterns.) The results for the homo-octahedral family are in agreement with those of Smith and Yoder (1956).

As shown above, real structures significantly influence the distribution of intensities compared with the corresponding Pauling model. Therefore, the calculation of XRD patterns was repeated for the following MDO polytypes of muscovite using idealized chemical composition and atomic coordinates resulting from the refinements of their structures: $1M_A$-I,1 (Sidorenko *et al.*, 1975), $2M_A$-II,1 (Güven, 1971), $2M_B$-III,1 (Zhoukhlistov *et al.*, 1973), and $3T_A$-IV,1 (Güven and Burnham, 1967). Their XRD powder patterns are shown in Figure 6 and listed in Table 11. A comparison with analogous patterns in Figure 5 reveals significant differences in the distribution of intensities. The differences suggest that identification of polytypes is more reliable when identification powder patterns are calculated using atomic coordinates derived from real structures. This should be kept in mind when working with micas having high values of the tetrahedral-rotation angle α, as well as with paragonite which has one of the highest values of α among the micas. Accordingly, the identification powder patterns of parago-

Table 11. Calculated transmission diffraction powder patterns of selected MDO polytypes of muscovite corresponding to randomly oriented aggregate (R) and oblique-texture geometry (ν_0 = 90°, ν_0 = 55°) for highly oriented aggregates.[1]

	$1M_A$-I,1				$2M_A$-II,1				$2M_B$-III,1				$3T_A$-IV,1			
		I_{rel}				I_{rel}				I_{rel}				I_{rel}		
d (Å)	hk*l*	R	90°	55°	hk*l*	R	90°	55°	hk*l*	R	90°	55°	hk*l*	R	90°	55°
9.91–9.99	001	46		2	002	53		3	002	62		3	003	58		6
4.95–4.99	002	22			004	23		2	004	29		2	006	26		3
4.45–4.48	020	63	100	12	020	82	93	56	110	83	88	39	100	75	91	40
					110				$\bar{1}11$				101			
					$\bar{1}11$											
					021											
4.34	$\bar{1}11$	36	42	19					$\bar{2}02$	25	21	18				
4.29					111	19	15	22					102			9
4.27									111	29	22	25				
4.08–4.10	021	27	19	22	022	15	8	24					103	22	13	24
3.96					112	11	4	19								
3.86–3.88					$\bar{1}13$	41	14	74	$\bar{1}13$	36	12	49	104	56	20	72
3.78–3.79	111	6	2	6					202	8	2	12				
3.73					023	42	11	78								
3.60–3.65	$\bar{1}12$	100	29	100					$\bar{2}04$	67	14	96	105	49		66
3.57					113	7	1	11								
3.49					$\bar{1}14$	57	10	100	$\bar{1}14$	72	12	100				
3.31–3.34	022	50	6	31	024	66	5	67	006	44		5	106	100		100
	003				006								009			
3.18–3.20					114	54	6	83	114	62	6	77				
3.10–3.13					$\bar{1}15$	8	1	12	$\bar{1}15$	11	1	13	107	63		74
3.04	112	93	10	77					204	54	4	62				
2.93–2.99					025	54	4	73	$\bar{2}06$	15	1	16				
2.90	$\bar{1}13$	28	3	21												
2.85–2.88					115	36	3	45	115	37	2	38	108	69		72
2.79–2.80					$\bar{1}16$	29	2	34	$\bar{1}16$	37	2	36				
2.66–2.68	023	36	4	22									109	9		11
2.59					130	49	55						$\bar{1}\bar{1}1$	44	55	22
					$\bar{1}31$											
					200			80								
2.57–2.56	130	68	96	24	116	100	100		$\bar{3}12$	100	100	53	112	86	100	49
	$\bar{1}31$				$\bar{2}02$				021							
2.52									$\bar{1}17$	13		8				
2.48–2.50	004	15	10	6	$\bar{1}17$	12	0	9	022	12			00,12	10		5
	$\bar{2}02$				008				008							
2.46					$\bar{1}33$	22	16	28								
2.43–2.44	113	16	13	10	202	15	10	20	$\bar{3}14$	28	17	27	$\bar{1}\bar{1}4$	28	22	24
	131				027											
2.41									023	24	14	25				
2.38–2.39	$\bar{1}32$	21	16	16	$\bar{2}04$	27	15	42	312	25	13	28	115	28	17	29
					133				$\bar{2}08$							
2.33–2.35	$\bar{1}14$	16	9	13					$\bar{3}15$	5	2	5				
	201															
2.30									024	8	4	10				
2.27									313	8	4	9				
2.24–2.25	$\bar{2}21$	13	20	4	040	11	12	13	$\bar{2}21$	15	16	6	200		6	
	040				$\bar{2}21$				$\bar{4}02$							
					220				220							
					041											
					$\bar{1}35$											

[1] For calculations the real geometry of crystal structures in Figure 6 and idealized chemical composition were used. The indexing refers to the actual unit cells.

nite polytypes were calculated using the following idealized chemical composition

$$Na_{0.9}K_{0.1}(Al_{2.0})(Si_{3.0}Al_{1.0})O_{10}(OH)_2$$

and the following atomic coordinates resulting from the refinements of their structures: $1M_A$-I,1 (Soboleva *et al.*, 1977), $2M_A$-II,1 (Sidorenko *et al.*, 1977b), and $3T_A$-IV,1 (Sidorenko *et al.*, 1977a). The results of the calculations are given in Table 12.

Oblique-texture geometry. From the general features of method (3) described above it follows that the individual superposition-structure reflections and the

https://doi.org/10.1346/CCMN.1986.0340107 Published online by Cambridge University Press

Table 12. Calculated transmission diffraction powder patterns of selected MDO polytypes of paragonite corresponding to randomly oriented aggregate (R) and oblique-texture geometry ($\nu_0 = 90°$, $\nu_0 = 55°$) for highly oriented aggregates.[1]

	$1M_A$-I,1				$2M_A$-II,1				$3T_A$-IV,1			
		I_{rel}				I_{rel}				I_{rel}		
d (Å)	hkl	R	90°	55°	hkl	R	90°	55°	hkl	R	90°	55°
9.66–9.57	001	55		3	002	70		6	003	45		7
4.83–4.79	002	37		2	004	31		3	006	21		3
4.45–4.33	020	87	100	25	110		73		100	73	76	47
	110				$\bar{1}11$			99	101			
					021	100	100					
4.28–4.24	$\bar{1}11$	59	44	52	111			26	102	16		14
4.13					$\bar{1}12$	11	7	20				
4.04	021	15	8	18	022	18	9	38				
3.94					112	5	2	10				
3.79–3.77	111	3		3	$\bar{1}13$	23	7	57	104	18		29
3.66					023	16	4	40				
3.51	$\bar{1}12$	67	12	93					105	33		56
3.37					$\bar{1}14$	29	4	66				
3.27–3.26	022	26	3	28	024	42	4	80	106	65		100
3.22–3.20	003	73		6	006	84		2				
3.19–3.17					114	53	5	100	009	70		16
3.03–3.01	112	87	7	100	$\bar{1}15$	4		6	107	46		67
2.92					025	42	3	77				
2.83					115	29	2	50				
2.79	$\bar{1}13$	20		19					108	47		61
2.69					$\bar{1}16$	22	2	33				
2.60	023	39		31					109	22		22
2.56–2.55	103	45	46	22	200	42	43		111	44	46	27
	$\bar{2}01$				$\bar{1}13$			98				
2.53	200	100	99	58	116	93	86		$\bar{1}\bar{1}2$	100	100	69
	$\bar{1}31$				131							
					$\bar{2}02$							
2.43					202	41	27	71				
2.42	113				$\bar{1}33$				114	53	35	62
	131	70	45	69	$\bar{1}17$	51	30	88				
	$\bar{2}02$											
2.35–2.34	201	24	12	28	133	34	17	68	$\bar{1}\bar{1}5$	34	18	44
	$\bar{1}32$				027							
					$\bar{2}04$							
2.25–2.22	$\bar{1}14$	4		3	$\bar{2}21$	5	4					
	$\bar{2}21$	5	4	3	220							
2.18–2.17	132	16	5	21	204		5	21	117	17		27
	203	15	6	13	221	23						
	041				$\bar{1}35$		7	55				
					042							
2.14–2.12					$\bar{2}23$	8	5	14	204	2		9
					222							
2.10–2.09					043	40	11	96	$\bar{1}\bar{1}8$	43	9	74
					135							
2.08–2.06	$\bar{1}33$	42	12	57	$\bar{2}06$	19	4	46				
	221				223	6	3					
2.02	042	3		4	044	7	3	15	206	2		9
1.98					$\bar{2}25$	5		7				
					$\bar{1}19$							

[1] For calculations the real geometry of crystal structures given by Soboleva *et al.* (1977), Sidorenko *et al.* (1977b) and Sidorenko *et al.* (1977a) for $1M_A$-I,1, $2M_A$-II,1, $3T_A$-IV,1, respectively and idealized chemical composition were used. The indexing refers to the actual unit cells.

MDO-group reflections cannot be enhanced separately. Thus, compromise ν_0 angle which would lead to XRD patterns *typical* for individual polytypes was found experimentally. Several attempts with different ν_0 angles led eventually to the value $\nu_0 = 55°$ which turned out to be the best choice. The identification powder patterns were thus calculated using this value.

The results of calculations for muscovite are given in Figure 7 and Table 11 and for paragonite in Table 12. To facilitate mutual comparisons, they are given for $\nu_0 = 55°$ and $\nu_0 = 90°$ as well as for the random-orientation geometry (R). It can be seen that, as far as identification of polytypes is concerned, the possibilities of the oblique-texture geometry after Krinari (1975)

https://doi.org/10.1346/CCMN.1986.0340107 Published online by Cambridge University Press

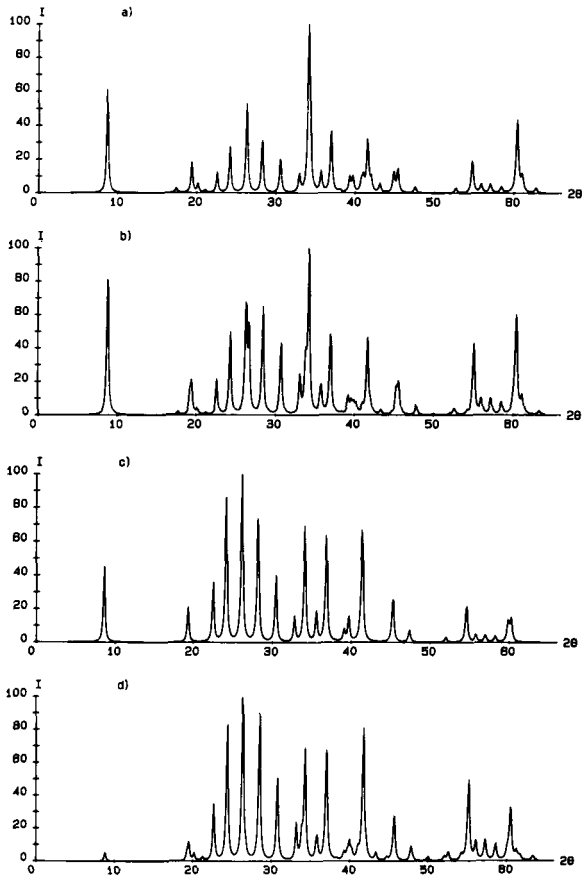

Figure 8. Diffraction patterns of $1M_A$-I phlogopite (conditions: diffractometer, transmission, Cu-radiation): (a) experimental pattern from sample with randomly oriented crystallites, (b) calculated pattern for sample with randomly oriented crystallites and for the real geometry of crystal structure given by Hazen and Burnham (1973), (c) experimental oblique texture pattern for $\nu_0 = 55°$ and sample with highly oriented crystallites, (d) calculated oblique texture pattern for $\nu_0 = 55°$, real geometry of crystal structure, as mentioned in (b) and for sample with highly oriented crystallites.

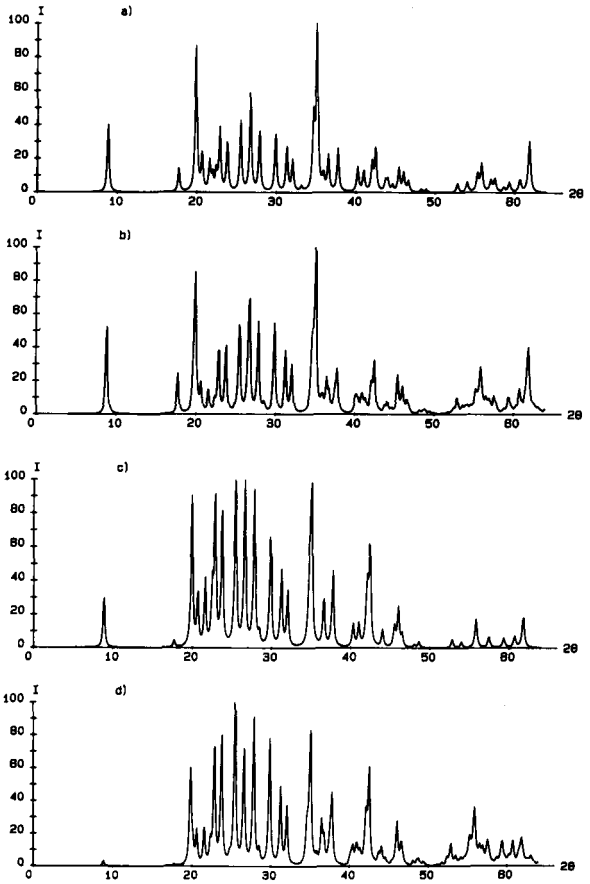

Figure 9. Diffraction patterns of $2M_A$-II,1 muscovite (conditions: diffractometer, transmission, Cu-radiation): (a) experimental pattern from sample with randomly oriented crystallites, (b) calculated pattern for sample with randomly oriented crystallites and for the real geometry of crystal structure given by Güven (1971), (c) experimental oblique texture pattern for $\nu_0 = 55°$ and sample with highly oriented crystallites, (d) calculated oblique texture pattern for $\nu_0 = 55°$, real geometry of crystal structure, as mentioned in (b) and for sample with highly oriented crystallites.

and of the random-orientation geometry are about the same.

Examples

To demonstrate the identification of mica polytypes by transmission methods (2) and (3), three samples of natural micas were chosen: phlogopite from Korea, muscovite from Strzegom (Poland) and paragonite from the Urals (U.S.S.R.). The self-supporting specimens with random orientation of crystallites were prepared on an X-ray transparent Mylar foil. The textured specimens were prepared by adding a fixed volume of a suspension containing a determined mass of the investigated powder (in the dry state) onto a well-stretched Mylar foil sealed in a glass tube container. The suspension was allowed to settle onto the foil, and supernatant water was sucked out or dried in vacuum at $\leq$40°C. After drying, the aggregate was separated from the glass tube and mounted in a standard window.

A comparison of the calculated and experimental diffraction patterns is given in Figures 8, 9, and 10 for phlogopite, muscovite, and paragonite, respectively. Note that the experimental patterns have been reproduced via computer in order to bring them on the same scale as the calculated ones. A close similarity of observed and calculated patterns is evident at once and indicates that the phlogopite is the $1M_A$-I polytype, the moscovite is the $2M_A$-II,1 polytype, and the paragonite is the $3T_A$-IV,1 (or $3T_A$-IV,2) polytype.

ACKNOWLEDGMENTS

The authors are greatly indebted to Dr. S. Ďurovič for critical reading of the work and for helpful discussions. The authors thank Dr. Bielkovskii for a sample

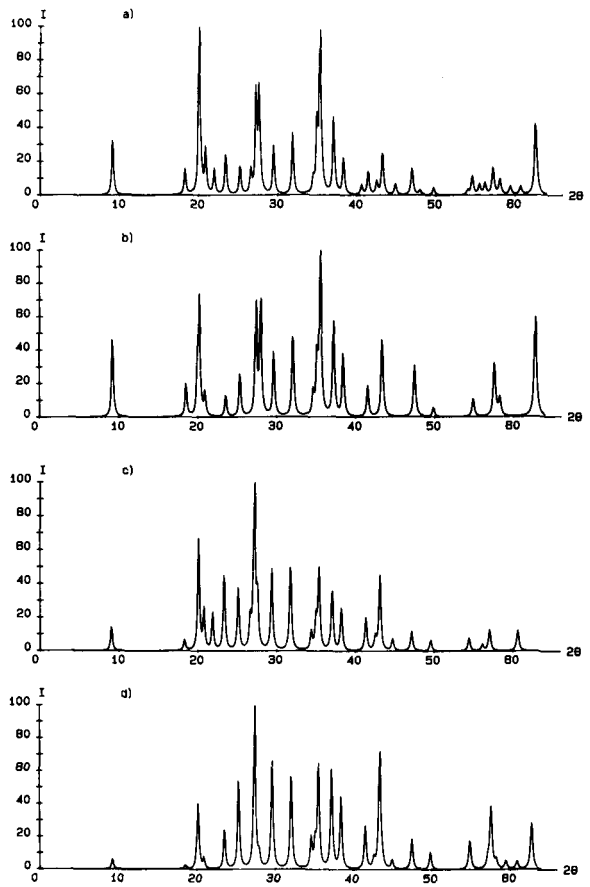

Figure 10. Diffraction patterns of $3T_A$-IV,1 paragonite (conditions: diffractometer, transmission, Cu-radiation): (a) experimental pattern from sample with randomly oriented crystallites, (b) calculated pattern for sample with randomly oriented crystallites and for the real geometry of crystal structure given by Sidorenko *et al.* (1977a), (c) experimental oblique texture pattern for $\nu_0 = 55°$ and sample with highly oriented crystallites, (d) calculated oblique texture pattern for $\nu_0 = 55°$, real geometry of crystal structure as mentioned in (b) and for sample with highly oriented crystallites.

of paragonite, Dr. Kozlowski for a sample of phlogopite and Mr. Pelc for a sample of muscovite.

REFERENCES

Backhaus, K.-O. and Ďurovič, S. (1984) Polytypism of micas. I. MDO polytypes and their derivation: *Clays & Clay Minerals* **32,** 453–463.

Baronnet, A., Pandey, D., and Krishna, P. (1981) Application of the faulted matrix model to the growth of polytype structures in mica: *J. Crystal Growth* **52,** 963–968.

Croche, R. (1976) Étude expérimentales et théoriques des corrections d'aberration instrumentales d'un diagramme de diffraction des rayons X: *Thèse presentée à la Conservatoire Nationale des Arts et Mêtiers,* Paris, 128 pp.

Dornberger-Schiff, K., Backhaus, K.-O., and Ďurovič, S. (1982) Polytypism of micas: OD interpretation, stacking symbols, symmetry relations: *Clays & Clay Minerals* **30,** 364–374.

Ďurovič, S., Weiss, Z., and Backhaus, K.-O. (1984) Polytypism of micas. II. Classification and abundance of MDO polytypes: *Clays & Clay Minerals* **32,** 464–474.

Guggenheim, S. (1981) Cation ordering in lepidolite: *Amer. Mineral.* **66,** 1221–1232.

Guggenheim, S. and Bailey, S. W. (1977) The refinement of zinnwaldite-1*M* in subgroup symmetry: *Amer. Mineral.* **62,** 1158–1167.

Guinier, A., Bokij, G. B., Boll-Dornberger, K., Cowley, J. M., Ďurovič, S., Jagodzinski, H., Krishna, P., De Wolf, P. M., Zvyagin, B. B., Cox, D. E., Goodman, P., Hahn, Th., Kuchitsu, K., and Abrahams, S. C. (1984) Nomenclature of polytype structures: Report of the International Union of Crystallography Ad-Hoc Committee on the Nomenclature of Disordered, Modulated and Polytype Structures: *Acta Crystallogr.* **A40,** 399–404.

Güven, N. (1971) The crystal structure of $2M_1$ phengite and $2M_1$ muscovite: *Z. Kristallogr.* **134,** 196–212.

Güven, N. and Burnham, C. W. (1967) The crystal structure of 3*T* muscovite: *Z. Kristallogr.* **125,** 163–183.

Hazen, R. M. and Burnham, C. W. (1973) The crystal structures of one-layer phlogopite and annite: *Amer. Mineral.* **58,** 889–900.

Krinari, G. A. (1975) On possibilities of using the oriented preparations of clay minerals for registration of non-basal X-ray diffractions: in *Kristallokhimiya Mineralov i Geologicheskie Problemy,* A. G. Kossowskaya, ed., Nauka, Moscow, 132–138 (in Russian).

Plançon, A., Rousseaux, F., Tchoubar, D., Tchoubar, C., Krinari, G. A., and Drits, V. A. (1982) Recording and calculation of *hk* rods intensities in case of diffraction by highly oriented powders of lamellar samples: *J. Appl. Crystallogr.* **15,** 509–512.

Ross, M., Takeda, H., and Wones, D. R. (1966) Mica polytypes: systematic description and identification: *Science* **151,** 191–193.

Sidorenko, O. V., Zvyagin, B. B., and Soboleva, S. V. (1975) Refinement of the crystal structure of dioctahedral mica 1*M*: *Kristallografiya* **20,** 543–549 (in Russian).

Sidorenko, O. V., Zvyagin, B. B., and Soboleva, S. V. (1977a) Crystal structure of paragonite 3*T*: *Kristallografiya* **22,** 976–981 (in Russian).

Sidorenko, O. V., Zvyagin, B. B., and Soboleva, S. V. (1977b) Refinement of the crystal structure of paragonite $2M_1$ by high-voltage electron diffraction: *Kristallografiya* **22,** 971–975 (in Russian).

Soboleva, S. V., Sidorenko, O. V., and Zvyagin, B. B. (1977) Crystal structure of paragonite 1*M*: *Kristallografiya* **22,** 510–514 (in Russian).

Smith, J. V. and Yoder, H. S. (1956) Experimental and theoretical studies of the mica polymorphs: *Mineral. Mag.* **31,** 209–235.

Weiss, Z., Krajíček, J., Smrčok, L., and Fiala, J. (1983) A computer X-ray quantitative phase analysis: *J. Appl. Crystallogr.* **16,** 493–497.

Zhoukhlistov, A. P., Zvyagin, B. B., Soboleva, S. V., and Fedotov, A. F. (1973) The crystal structure of the dioctahedral mica $2M_2$ determined by high-voltage electron diffraction: *Clays & Clay Minerals* **21,** 465–470.

Zvyagin, B. B. (1967) *Electron Diffraction Analysis of Clay Mineral Structures:* Plenum Press, New York, 364 pp.

Zvyagin, B. B., Vrublevskaya, Z. V., Zhoukhlistov, A. P., Sidorenko, O. V., Soboleva, S. V., and Fedotov, A. F. (1979) *High-Voltage Electron Diffraction in the Investigation of Layered Minerals:* Nauka, Moscow, 224 pp. (in Russian).

(Received 31 August 1984; accepted 30 May 1985; Ms. 1409)